International Journal of Solids and Structures 48 (2011) 2458–2466

Contents lists available at ScienceDirect

International Journal of Solids and Structures

journal homepage: www.elsevier.com/locate/ijsolstr

A continuum damage model for the high-cycle fatigue life prediction of styrene-butadiene rubber under multiaxial loading

G. Ayoub [a,b], M. Naït-Abdelaziz [a,b,*], F. Zaïri [a,b,*], J.M. Gloaguen [a,c], P. Charrier [d]

[a] Univ Lille Nord de France, F-59000 Lille, France
[b] Université Lille 1 Sciences et Technologies, Laboratoire de Mécanique de Lille (LML), UMR CNRS 8107, F-59650 Villeneuve d'Ascq, France
[c] Université Lille 1 Sciences et Technologies, Unité Matériaux Et Transformations (UMET), UMR CNRS 8207, F-59650 Villeneuve d'Ascq, France
[d] Groupe Trelleborg, Société Modyn, Service Recherche et Innovations, Zone Industrielle Nantes Carquefou, BP 419, 44474 Carquefou Cedex, France

ARTICLE INFO

Article history:
Received 7 February 2011
Received in revised form 17 March 2011
Available online 22 April 2011

Keywords:
Elastomeric-like materials
Multiaxial fatigue life prediction
Continuum damage mechanics
Cracking energy density

ABSTRACT

In the present contribution, the relationship between the fatigue life of styrene-butadiene rubber (SBR) and the stretch amplitude was established. Focusing on the multiaxial loading effect on the life duration of SBR, experimental tests were conducted using cylindrical specimens subjected to tension and torsion loadings under constant and variable amplitudes. Based upon the continuum damage mechanics approach, a three-dimensional model was derived and coupled with the cracking energy density criterion to predict the fatigue life of SBR. The capabilities of the model, which requires only three damage parameters to be identified, were analysed and a good agreement between predicted values and experimental data were clearly highlighted for tension and torsion loadings both in constant and variable amplitudes.

1. Introduction

Elastomeric materials are used in industrial applications such as tires, hoses, dampers for the automotive/aircraft industry. These applications require a good performance under static loading and durability under cyclic loading. Rubber components of mechanical structures could be subjected to variable loads leading to fatigue fracture. Early in the product development process, engineers need simulation software capable of predicting stress and strain histories in the purpose of modelling and designing for mechanical fatigue. Therefore, understanding the damaging processes and predicting the life duration under multiaxial loading is a primary consideration for industrial design.

In a very useful background paper, Mars and Fatemi (2002) have widely reported the main approaches used to describe the fatigue of rubbers. As for most of materials, the fracture of rubbers under fatigue loading conditions could be described by two main mechanisms: nucleation of defects and propagation until complete failure of nucleated cracks. In the fatigue life duration of a rubber component, the time required to nucleate a defect of a given size and that necessary to propagate a defect until complete fracture depend on many parameters such as the geometry of the rubber specimen, the loading conditions, etc. So, generally, these two stages in fatigue investigation are often separately studied, although some authors have tried to give a unified approach but based on crack propagation.

Concerning the fatigue crack propagation, the fatigue life is defined as the number of cycles required by a pre-existing crack to grow until fracture. The strain energy release rate early introduced by Griffith (1920) and extended by Rivlin and Thomas (1953) to fracture of rubbers is generally used as a governing parameter to describe the crack growth and to build empirical laws (as that developed by Paris for metals but using the stress intensity factor).

When dealing with the crack nucleation, the fatigue life is generally taken as the number of cycles required to create a crack of a given size. It is often related to macroscopic mechanical quantities (such as stresses or strains) which are taken as indicators of fatigue loadings. Following the pioneering work of Wöhler (1867) for steels, Cadwell et al. (1940) extended this kind of approach to rubber components. The three most widely used predictor parameters for rubber fatigue are: (i) the maximum principal strain, (ii) the maximum principal Cauchy stress and (iii) the strain energy density (SED). More recently, (iv) the cracking energy density (CED) criterion proposed by Mars (2001, 2002) and (v) the criterion based on the configurational mechanics (Eshelby, 1951) – the Eshelby stress tensor – proposed by Verron and Andriyana (2008) constitute more elaborated approaches to investigate fatigue of elastomeric-like materials.

In the remainder of the introduction, literature results regarding these predictor parameters are briefly summarized.

* Corresponding authors at: Univ Lille Nord de France, F-59000 Lille, France. Tel.: +33 328767460; fax: +33 328767301.
E-mail addresses: moussa.nait-abdelaziz@polytech-lille.fr (M. Naït-Abdelaziz), fahmi.zairi@polytech-lille.fr (F. Zaïri).

0020-7683/$ - see front matter © 2011 Elsevier Ltd. All rights reserved.
doi:10.1016/j.ijsolstr.2011.04.003

Nomenclature

N_f	number of cycles to failure
N_i	number of cycles performed for block i
ω, ω_i	frequency, frequency for block i
δ, δ_{max}, δ_{min}	axial displacement, maximum, minimum
θ, θ_{max}, θ_{min}	twist angle, maximum, minimum
HL	δ for block i is higher than block $i+1$
LH	δ for block i is lower than block $i+1$

1.1. Maximum principal strain

The maximum tensile strain generally governs the crack nucleation which occurs in a perpendicular plane to its direction. The first fatigue life studies in rubber noticed that it is possible to develop an empirical criterion based on the description of the number of cycles until failure as a function of alternation strain and minimum strain. Cadwell et al. (1940) and Fielding (1943) highlighted that the fatigue life of a natural rubber (NR), under axial and shear tests, could be improved by increasing the minimum stretch. The fatigue life under simple and equibiaxial tension tests was investigated, more recently, by Roberts and Benzies (1977) and Roach (1982). It was observed that the fatigue life was longer in simple tension than in equibiaxial tension tests when plotted against the maximum strain ratio. Ro (1989) re-analysed the data of these latest studies and concluded that the strain is not an optimal parameter for unifying simple and equibiaxial tension tests.

1.2. Maximum principal Cauchy stress

Some authors have proposed to link the fatigue life of elastomeric-like materials to the maximum principal Cauchy stress (André et al., 1999; Abraham et al., 2005; Saintier et al., 2006). Especially, André et al. (1999) pointed out that the maximum principal Cauchy stress could be taken as an indicator of fatigue and showed that the cracks orientation is perpendicular to its direction.

1.3. Strain energy density

The development of the nucleation life approach in elastomeric-like materials was motivated by the success of fracture mechanics in the 1960s. Especially, the SED started to be used as a predictor parameter for fatigue crack nucleation. Gent et al. (1964), Lee and Moet (1993) and Aït-Hocine et al. (1998) found that, under certain conditions, the energy release rate is proportional to the SED and could be written in a multiplicative form of the SED and the crack size. However, it was shown by Roberts and Benzies (1977) and Roach (1982) that the SED could not unify Wöhler curves for uniaxial and equibiaxial tension tests while Ro (1989) and Abraham et al. (2005) found that the SED is a better predictor than those previously described. Whatever its capability as an indicator of fatigue damage, the main drawback of the SED is its inefficiency to predict the crack nucleation plane.

1.4. Cracking energy density

Assuming that only a certain part of the SED is available for flaw growth, Mars (2001, 2002) introduced the CED W_c as a candidate for predicting both nucleation and crack orientation. Using the infinitesimal strain framework, Mars (2001, 2002) developed this quantity by introducing the increment of energy available to be released on a given material plane of normal vector $\mathbf{r}$. This latter is defined as the dot product of the Cauchy traction vector $\boldsymbol{\sigma}\mathbf{r}$ ($\boldsymbol{\sigma}$ being the Cauchy stress tensor) with the increment of strain $d\boldsymbol{\varepsilon}$ in the $\mathbf{r}$-direction. The increment of CED is given by (Mars, 2001, 2002): $dW_c = (\boldsymbol{\sigma}\mathbf{r})(d\boldsymbol{\varepsilon}\mathbf{r}) = \mathbf{r}\boldsymbol{\sigma}d\boldsymbol{\varepsilon}\mathbf{r}$. The material critical plane depicted by its normal $\mathbf{r}$ which maximizes the CED at a given point is supposed to be the most probable plane where the crack can occur for a given loading. Mars (2001, 2002) extended the previous expression to finite strains but the proposed formulation is questionable since the definition of the normal vector was not completely clarified (Zine, 2006; Zine et al., 2006).

1.5. Eshelby stress tensor

It was in the pioneering work of Eshelby (1951) where the theory of configurational mechanics was first introduced and the concept of the energy–momentum tensor and configurational forces in continuum mechanics first developed. In particular, the J integral (Rice, 1968), often used as a governing parameter in nonlinear fracture mechanics, was derived from this concept. This theory was then extended to finite strains by Chadwick (1975). Maugin (1993) considered that configurational mechanics as an extension of the continuum mechanics and named it the eshelbian mechanics. Most of the works focus on the application of the configurational mechanics to fracture mechanics. Few studies were interested into the properties of the configurational stress tensor. Motivated by microscopic mechanisms induced by fatigue, Verron and Andriyana (2008) proposed a criterion for the crack nucleation prediction in rubbers based on the configurational mechanics.

1.6. Damage accumulation rules

The fatigue life prediction can be therefore approached by using a mechanical quantity as a predictor (like those above described). This kind of approach works more or less especially when focusing on fatigue life of rubbers under constant amplitude loading conditions. When dealing with variable loading a damage rule is required (Miner, 1945).

In this case, the rules are generally based on experimental results obtained for specific loading cases and materials. Because simple, since it is a linear law, the Miner rule (Miner, 1945) is widely used. This rule implies, in the case of variable loadings, that the order in which loads are applied is not significant. Klenke and Beste (1987) were the first to apply the Miner rule to predict fatigue life involving rubbers. Sun et al. (2000) found that the Miner rule was not applicable under multilevel loadings. Most recently, Harbour et al. (2008) investigated the effect of variable amplitude loading conditions on the fatigue life of multiaxial rubber specimens, using the Miner rule, for two types of materials (NR and SBR). They found that the Miner rule predicts reasonably well the fatigue life duration of NR under variable amplitude loadings. On the contrary, it was not able to predict the fatigue life duration of SBR under the same loading conditions.

Another way is to calculate the damage accumulation cycle by cycle using the continuum damage mechanics (CDM) concept coupled with a fatigue predictor. Originally, the theory of continuum damage was introduced by Kachanov (1958) to explain the process of continuous deterioration of materials subjected to creep. The success of this creep damage modelling has prompted its extension to fatigue damage. Later, several contributions used the CDM approach to predict the fatigue damage life of materials (Lemaitre and Chaboche, 1994). The CDM theory was recently applied to NR by Wang et al. (2002) to describe the fatigue life as a function of the

strain amplitude. The damage evolution was derived using a first-order Ogden SED (Ogden, 1972) and analytically developed by only considering tensile cyclic loading under constant stretch amplitude. Ayoub et al. (2010) recently improved the CDM model of Wang et al. (2002) by adopting a generalized form of the Ogden SED, in one hand, and by achieving the theoretical developments under multiaxial loading, in another hand. The purpose of the present contribution is to improve the capabilities of the model.

1.7. Scope of the present work

Using the CDM framework our purpose is to develop a new tool able to predict the fatigue life of rubbers under multiaxial and multilevel loading. For this purpose, we will incorporate the Mars (2001, 2002) CED in the CDM theory written in a general form. The outline of the present paper is as follows. Section 2 is devoted to the experimental investigation we have achieved on a representative elastomeric-like material (styrene-butadiene rubber – SBR). In Section 3, the developed three-dimensional CDM criterion is fully described and exercised on the experiments. Section 4 presents an improvement of the CDM model by combining it to the CED criterion. The required damage parameters were identified on the tensile fatigue tests and then the new model was validated by comparing its prediction with the experimental data corresponding to multiaxial loading under constant and variable amplitudes. Finally, remarks and conclusions are given in Section 6.

2. Experiments

2.1. Material and specimen

The material under investigation is a sulfur-vulcanized SBR filled with 34 phr of carbon black. The specimens were supplied by the Trelleborg Group. The material formulation provided by the manufacturer is given in Table 1. The main specimen geometric features are given in Fig. 1. The specimens are axisymmetric and the predominant fatigue crack is initiated in the mid-plane in which the local deformation state is the highest. Obviously, the specimen curvature radius is large enough to minimize the stress triaxiality effects (Aït-Hocine et al., 2011).

Dynamic fatigue tests were run on a traction-torsion Instron-8874 servo hydraulic testing device, at room temperature under low frequencies from 3 up to 5 Hz. The cyclic loading mode was based upon a sine wave function. Displacement (or angle) and force data as functions of the time were recorded in a computer. All tests were achieved under controlled displacement (or angle), the amplitudes of which were selected in order to cover a wide range of fatigue lives.

2.2. Scheme of experimental fatigue tests and results

Both constant and variable amplitude signals were used with the multiaxial cylindrical samples. Various types of tests are graphically described in Fig. 2 where θ represents the torsion angle and δ the axial elongation. The tests A to C were achieved under a constant amplitude condition under tension, torsion or combined tension–torsion loadings until fatigue failure. Test A is a pure tension test with a minimum axial displacement of zero. Test B is a torsion test with a minimum twist angle of zero. Test C is a proportional loading path in which the axial displacement and the twist angle in phase starting both from zero. Test D is a variable amplitude signal consisting of a combination of constant amplitude loadings: two blocks with different maximum strain levels under axial loading. Tests conditions and cycle number until failure for load tests described in Fig. 2 are shown in Table 2 for the tests A, B and C and in Table 3 for variable amplitude tests D.

Table 1
Material formulation of SBR. All the ingredients are in phr (parts per hundred rubber).

Ingredients	Value
SBR	100
Zinc oxide	10
Processing oil	0
Carbon black	34
Sulfur	3
Stearic acid	3
Antioxidant	5
Accelerators	4.3

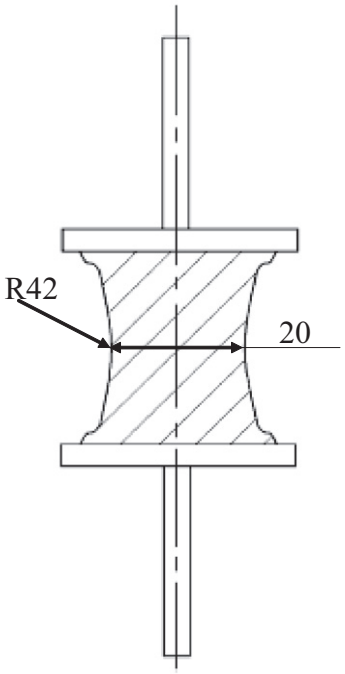

Fig. 1. Geometry and dimension of the sample.

The number of cycles to failure remains quite difficult to estimate. When cracks nucleate on the free surface, it is reasonable to take the fatigue life as the number of cycles corresponding to a crack length of 1 mm.

The evolution of the maximum axial load and torque with the cycle number is presented in Fig. 3. It can be observed that under constant displacement amplitude, the stress level decreases of about 50% after a short time, then it remains quite constant until the onset of crack nucleation. For the torsion test, the stress softening is more continuous until the complete failure. It was observed that the magnitude of the stress softening depends on the maximum applied displacement (or angle). The stress softening phenomenon within the first cycles may be associated with the rearrangement of the chains network (Ayoub et al., 2011) due to chains and links breakage.

3. A CDM model for the fatigue life prediction: formulation and results

In order to predict the fatigue life of SBR a CDM model based upon the effective stress concept introduced by Lemaitre and Chaboche (1994) is developed in this section. The proposed damage mechanics model is an extension for any kind of loading of that proposed by Wang et al. (2002).

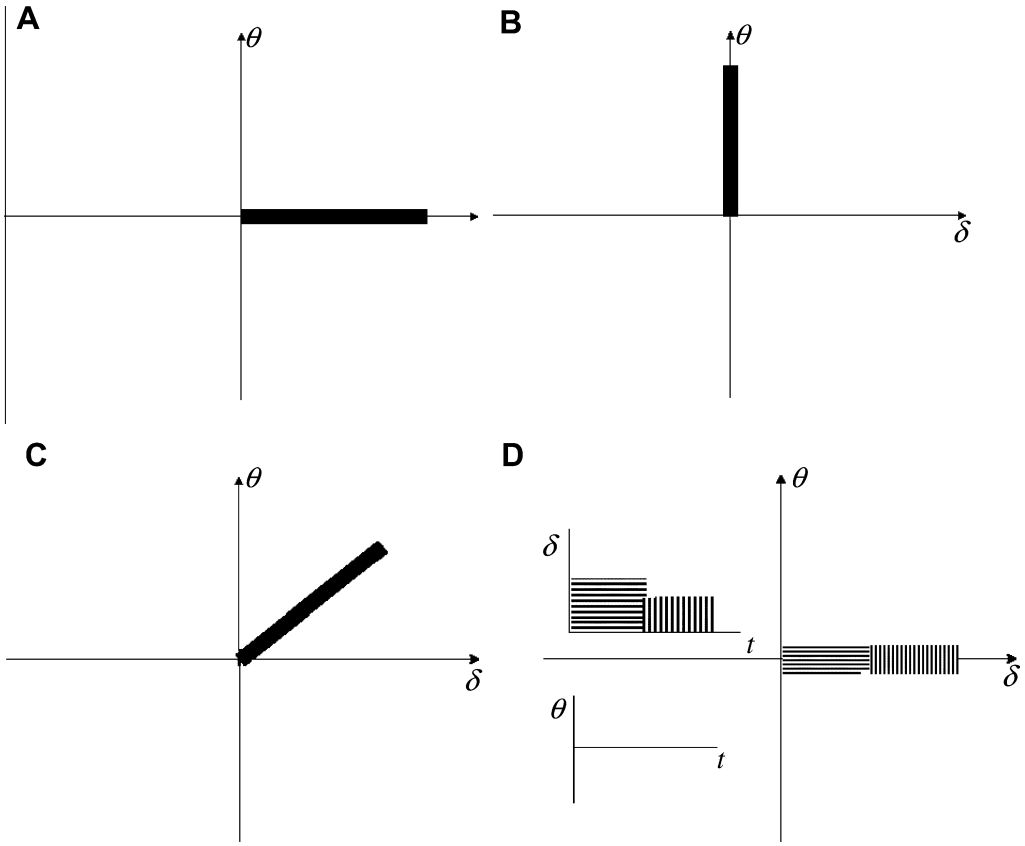

Fig. 2. Graphical description of various types of tests.

3.1. Multiaxial formulation of the CDM concept

The rubber material is assumed as an isotropic, homogeneous, incompressible and hyperelastic body. The model developed in this paper is based on the general damage mechanics framework for the hyperelasticity theory.

During the fatigue process, the initiation and propagation of microcracks occur through a continuous evolution of the damage. In the CDM approach, the main assumption is that, due to these microcracks, the net section contributing to the load transfer in a specimen or in a structure decreases with damage (Lemaitre and Chaboche, 1994). Using the effective stress concept in terms of second Piola–Kirchhoff principal stresses, the effective principal stresses $\widetilde{S}_i$ are related to the principal stresses S_i by:

$$\widetilde{S}_i = \frac{S_i}{(1-D)} \quad 1 \leqslant i \leqslant 3 \tag{1}$$

where D is a scalar defining the isotropic damage evolution and could be related to the evolution of the net section. The damage variable D is zero in the initial state (virgin material) and 1 for fracture (when a macroscopic crack is initiated).

In the isotropic damage mechanics framework, the damage kinetics is expressed as:

$$\dot{D} = -\frac{\partial \varphi^*}{\partial y} \tag{2}$$

in which y is the damage strain energy release rate and φ^* is the dissipation potential which can take the following form:

$$\varphi^* = \frac{A}{a+1}\left(\frac{-y}{A}\right)^{a+1} \tag{3}$$

where a and A are two damage parameters.

Elastomeric-like materials are generally described by hyperelastic laws derived from SED functions. The hyperelasticity theory has been addressed by numerous authors (see e.g. (Dorfmann and Muhr, 1999; Boyce and Arruda, 2000) for reviews and extensive discussions of constitutive models derived from this theory). The general formulation of the Ogden SED is employed in this paper to derive the damage strain energy release rate. The Ogden SED of an undamaged material, a function of the principal stretches λ_1, λ_2 and λ_3, is expressed as follows (Ogden, 1972):

$$W = \sum_{i=1}^{n} \frac{\mu_i}{\alpha_i}\left(\lambda_1^{\alpha_i} + \lambda_2^{\alpha_i} + \lambda_3^{\alpha_i} - 3\right) + \frac{9}{2}K(J^{1/3}-1)^2 \tag{4}$$

where μ_i and α_i are material parameters. $\mu = \sum_{i=1}^{n}\mu_i$ is the shear modulus, K is the bulk modulus and $J = \lambda_1\lambda_2\lambda_3$ is the Jacobian, equal to 1 for incompressible materials.

The damage strain energy release rate y is defined as:

$$-y = \frac{\partial W}{\partial D} \tag{5}$$

in which W is the SED function of the damaged material.

Because the SED function W of a damaged material is a function of the effective principal stresses $\widetilde{S}_i$, the damage strain energy release rate y can be written in the following form:

$$-y = \frac{\partial W(\widetilde{S}_i)}{\partial D} = \frac{\partial W}{\partial \lambda_1}\frac{\partial \lambda_1(\widetilde{S}_i)}{\partial D} + \frac{\partial W}{\partial \lambda_2}\frac{\partial \lambda_2(\widetilde{S}_i)}{\partial D} + \frac{\partial W}{\partial \lambda_3}\frac{\partial \lambda_3(\widetilde{S}_i)}{\partial D} \tag{6}$$

Differentiating of $\widetilde{S}_i$ in Eq. (1) with respect to the damage variable D leads to:

$$\frac{\partial \lambda_i(\widetilde{S}_i)}{\partial D} = \frac{\widetilde{S}_i}{(1-D)\frac{\partial \widetilde{S}_i}{\partial \lambda_i}} \quad 1 \leqslant i \leqslant 3 \tag{7}$$

Table 2
Fatigue life results of constant amplitude tests.

Test code	ω (Hz)	δ_{max}(mm)	δ_{min}(mm)	θ_{max}°)	θ_{min}°)	N_f
A	5	5.6	0.0	0.0	0.0	3000000
A	5	7	0.0	0.0	0.0	500000
A	5	8.4	0.0	0.0	0.0	160000
A	5	9.8	0.0	0.0	0.0	24000
A	5	11.2	0.0	0.0	0.0	19200
A	5	12.6	0.0	0.0	0.0	12564
A	5	14	0.0	0.0	0.0	6000
A	5	15.4	0.0	0.0	0.0	4300
A	5	16.8	0.0	0.0	0.0	3050
A	5	18.2	0.0	0.0	0.0	2200
A	5	19.6	0.0	0.0	0.0	1800
A	5	21	0.0	0.0	0.0	1350
A	5	22.4	0.0	0.0	0.0	1050
A	5	23.8	0.0	0.0	0.0	900
A	5	25.2	0.0	0.0	0.0	800
A	5	26.6	0.0	0.0	0.0	650
A	5	28	0.0	0.0	0.0	560
B	3	0.0	0.0	100	0.0	1100000
B	3	0.0	0.0	105	0.0	1000000
B	3	0.0	0.0	110	0.0	680000
B	3	0.0	0.0	115	0.0	400000
B	3	0.0	0.0	120	0.0	280000
B	3	0.0	0.0	125	0.0	200000
B	3	0.0	0.0	130	0.0	130000
B	3	0.0	0.0	135	0.0	100000
B	3	0.0	0.0	140	0.0	79000
B	3	0.0	0.0	145	0.0	68000
C	5	5.6	0.0	50	0.0	600000
C	5	8.4	0.0	50	0.0	60000
C	5	9.8	0.0	50	0.0	15000
C	5	14	0.0	50	0.0	4200
C	5	16.8	0.0	50	0.0	1776
C	5	19.6	0.0	50	0.0	1200
C	5	25.2	0.0	50	0.0	650
C	5	5.6	0.0	100	0.0	40000
C	5	9.8	0.0	100	0.0	10000
C	5	14	0.0	100	0.0	3080
C	5	16.8	0.0	100	0.0	1413
C	5	19.6	0.0	100	0.0	850
C	5	25.2	0.0	100	0.0	500

Table 3
Fatigue life results of variable amplitude tests ($N_f = N_1 + N_2$).

		Block 1			Block 2		
Test code		ω_1 (Hz)	δ_{max}(mm)	N_1	ω_2 (Hz)	δ_{max}(mm)	N_2
D1	LH	5	7	200000	5	11.2	11000
D1	LH	5	7	200000	5	8.4	82500
D2	HL	5	8.4	80000	5	7	118470
D2	LH	5	8.4	80000	5	11.2	10011
D2	LH	5	8.4	80000	5	14	3760
D3	HL	5	14	3250	5	7	100010
D3	HL	5	14	3250	5	11.2	15213
D3	LH	5	14	3250	5	16.8	950
D3	LH	5	14	3250	5	19.6	550
D3	LH	5	14	3250	5	22.4	450
D4	HL	5	16.8	1525	5	11.2	5000
D4	HL	5	16.8	1525	5	14	1070
D4	LH	5	16.8	1525	5	22.4	290
D5	HL	5	19.6	800	5	14	2875
D6	HL	5	22.4	525	5	11.2	13103
D6	HL	5	22.4	525	5	15	2140
D6	HL	5	22.4	525	5	16.8	1300

Using Eqs. (4), (6) and (7), the damage strain energy release rate y is defined as:

$$-y = \frac{S_{eq}}{1-D} \tag{8}$$

in which the term S_{eq} is an equivalent quantity of a stress:

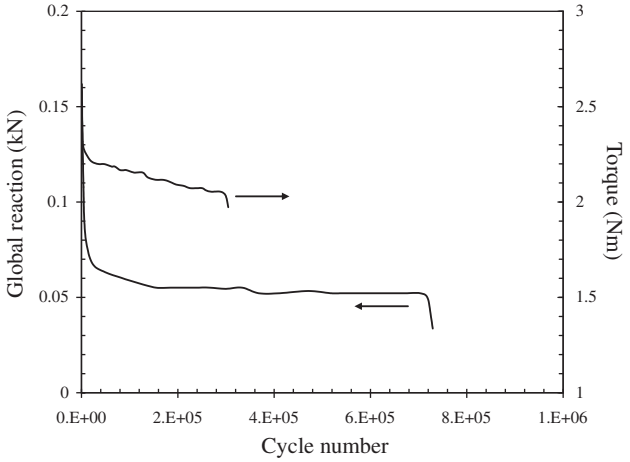

Fig. 3. Maximum load evolution under tension and torsion fatigue tests.

$$S_{eq} = \sum_{i=1}^{3} \frac{\widetilde{S}_i}{\frac{\partial S_i}{\partial \lambda_i}} \frac{\partial W}{\partial \lambda_i} = \sum_{i=1}^{3} \frac{\left(\sum_{j=1}^{n} \mu_j \lambda_i^{\alpha_j - 2} + p\lambda_i^{-2}\right)\left(\sum_{j=1}^{n} \mu_j \lambda_i^{\alpha_j - 1} + p\lambda_i^{-1}\right)}{\left(\sum_{j=1}^{n} \mu_j (\alpha_j - 2)\lambda_i^{\alpha_j - 3} + \frac{\partial p}{\partial \lambda_i}\lambda_i^{-2} - 2p\lambda_i^{-3}\right)} \tag{9}$$

where p is the hydrostatic pressure[1] which must be determined from the boundary conditions.

Combining Eqs. (2), (3) and (8), the damage kinetics can be expressed as follows:

$$\dot{D} = \left(\frac{S_{eq}}{A(1-D)}\right)^a \tag{10}$$

Under a cyclic loading condition, the damage rate could be linked to the number of cycles N and written as follows:

$$\frac{\partial D}{\partial N} = \left(\frac{S_{eq}}{A(1-D)}\right)^a \tag{11}$$

The damage variable D is zero for the virgin material i.e. $D = D_0 = 0$ when $N = N_0 = 0$. Integration of Eq. (11) gives the current damage value at the considered cycle:

$$\int_{D_0=0}^{D} (1-D)^a dD = \int_{N_0=0}^{N} \left(\frac{S_{eq}}{A}\right)^a dN \tag{12}$$

Therefore, the induced damage D due to N cycles is given by:

$$D = 1 - \left[1 - (1+a)\left(\frac{S_{eq}}{A}\right)^a N\right]^{\frac{1}{1+a}} \tag{13}$$

The evolution of the damage variable D as a function of the normalized fatigue life N/N_f is shown in Fig. 4. The fatigue life corresponding to damage reaching its maximum value 1, $D = D_f = 1$ and $N = N_f$ can be expressed in the following form:

$$N_f = \frac{A^a}{1+a} S_{eq}^{-a} \tag{14}$$

The identification of the damage parameters a and A of the CDM model for fatigue life prediction is allowed by linearization of Eq. (14):

[1] In the incompressible case, this term is introduced in the components of the stress. For example, the second Piola–Kirchhoff stress components in the principal directions are related to the SED in the following form: $S_i = \frac{1}{\lambda_i}\frac{\partial W}{\partial \lambda_i} - p\frac{1}{\lambda_i^2} 1 \leqslant i \leqslant 3$.

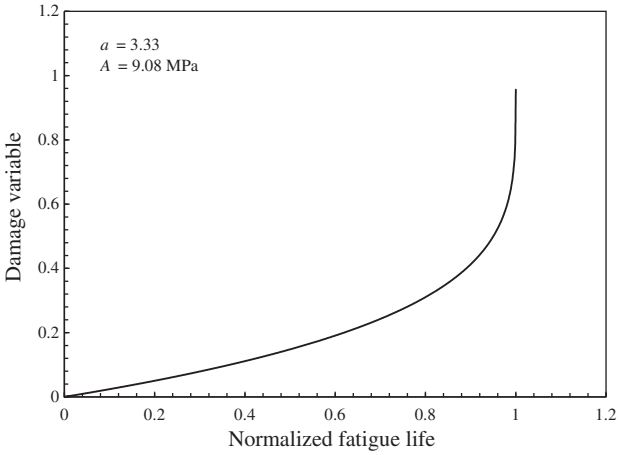

Fig. 4. Damage variable versus normalized fatigue life.

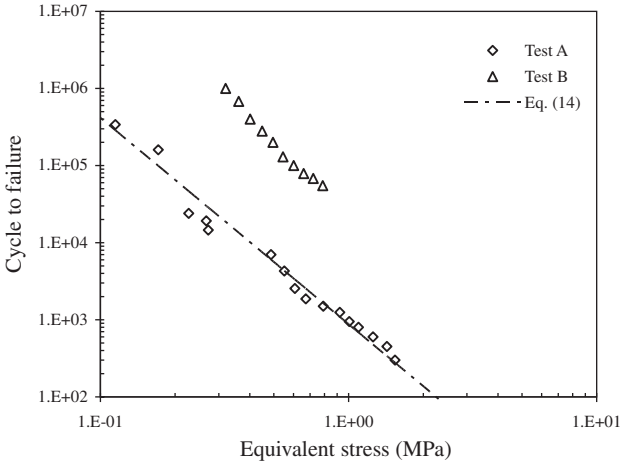

Fig. 6. Fatigue life of SBR in terms of the equivalent stress calculated using Eq. (9).

$$\log(N_f) = -a\log(S_{eq}) + \log\left(\frac{A^a}{1+a}\right) \tag{15}$$

In the case of variable amplitude loading conditions, the damage variable D_i at a given sequence i can be expressed using Eq. (13) written in the following manner:

$$D_i = 1 - \left[(1-D_{i-1})^{1+a} - (1+a)\left(\frac{S_{eq}}{A}\right)^a N_i\right]^{\frac{1}{1+a}} \tag{16}$$

For n blocks at different successive amplitude loadings, the fatigue life $N_f = N_n$ can be extracted from the following general equation:

$$\int_{D_0=0}^{D_f=1}(1-D)^a dD = \sum_{i=0}^{n-1}\int_{N_i}^{N_{i+1}}\left(\frac{S_{eq(i+1)}}{A}\right)^a dN \tag{17}$$

3.2. Comparison between model and experimental results

In this subsection, our experimental results are compared to the predictions given by the above-described model.

The intrinsic constitutive response of the SBR material during monotonic (tension and torsion) loading was experimentally determined and captured by the Ogden constitutive model. It is worth noticing that the so-called Mullins effect (stress-softening after one cyclic loading) was neglected. To this end, each sample was loaded until the maximum stretch amplitude encountered by the material during the fatigue loading, and the resulting sample was considered as the virgin material. It is found that a second-order Ogden expression adequately reproduces the response during both tension/compression and torsion tests of the studied SBR material (see Fig. 5). The material constant values determined from experiments are: $\mu_1 = 5.25$ MPa, $\mu_2 = 1.52 \times 10^{-2}$ MPa, $\alpha_1 = 2.14 \times 10^{-1}$ and $\alpha_2 = 4.06$. Note that the difference in the material constant values of this phenomenological model between Ayoub et al. (2010) and the present paper is due to the compression path which was added in the identification procedure.

The two damage parameters a and A are identified by using the least square method applied to Eq. (14). The tensile fatigue tests are used as the reference to determine these two parameters ($a = 2.68$ and $A = 13.12$ MPa). The fatigue life is then plotted in Fig. 6 as a function of the equivalent stress defined by Eq. (9). This figure clearly shows that the SED could not be taken as a fatigue indicator since it could not unify the experimental data corresponding to tension (A) and torsion (B) tests.

4. An improved CDM model for the fatigue life prediction

If referring to the fracture mechanics approaches, under uniaxial loading, the energy released due to crack propagation is proportional to the SED. More generally, in the case of multiaxial loading only a part of the SED contributes in the initiation mechanisms of a crack. Mars (2001, 2002) proposed a continuum mechanical parameter (see Appendix A for the details) – the CED parameter – providing the determination of the energy portion that contributes to damage the material under multiaxial fatigue. The increment of total SED dW can be thus additively split into a part that does not contribute to cracking dW_{nc} and the increment of CED dW_c:

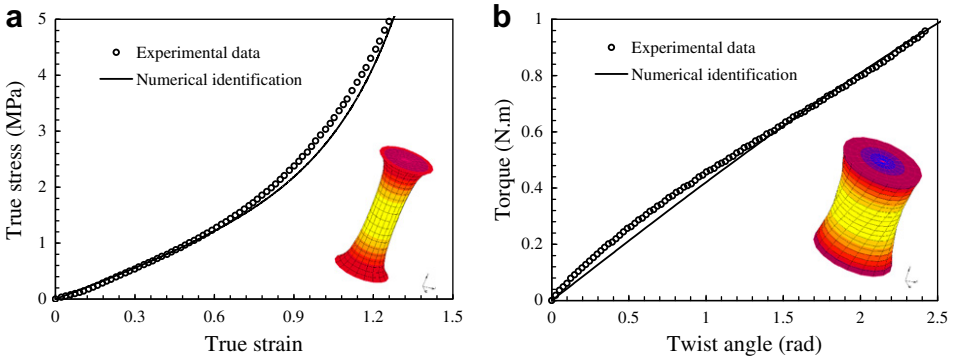

Fig. 5. Comparison between monotonic experimental data and Ogden model simulation for (a) uniaxial tension and (b) pure torsion loadings.

$$dW = dW_c + dW_{nc} \tag{18}$$

The expressions under finite strains of the increments of SED dW and CED dW_c are recalled in Eqs. (A.1) and (A.2) of Appendix A. The most probable plane where the cracking occurs corresponds to the material plane which maximizes the CED at a given point. Note that for a pure tension loading, the ratio W_c/W tends to one (Zine et al., 2006), in other words for this specific case all the SED contributes to cracking process.

Using the same framework than that used in Section 3.1 we propose to consider only the contribution of the CED to develop the multiaxial fatigue predictor. It is assumed that the CED W_c is a function of the effective principal stresses $\widetilde{S}_i$. Therefore, the damage strain energy release rate y is defined as:

$$-y = \frac{\partial W_c(\widetilde{S}_i)}{\partial D} = \frac{\partial W_c}{\partial \lambda_1}\frac{\partial \lambda_1(\widetilde{S}_i)}{\partial D} + \frac{\partial W_c}{\partial \lambda_2}\frac{\partial \lambda_2(\widetilde{S}_i)}{\partial D} + \frac{\partial W_c}{\partial \lambda_3}\frac{\partial \lambda_3(\widetilde{S}_i)}{\partial D} \tag{19}$$

where $\partial\lambda_i(\widetilde{S}_i)/\partial D\ 1 \leqslant i \leqslant 3$ are given by Eq. (7) and $\partial W_c/\partial \lambda_i\ 1 \leqslant i \leqslant 3$ are given by Eq. (A.7) of Appendix A.

A new formulation of the equivalent stress is thus provided:

$$S_{eq} = \frac{1}{(\cos^2\theta + B^{-2}\sin^2\theta)}\left(\frac{S_1^2\lambda_1\cos^2\theta}{\partial S_1/\partial\lambda_1} + \frac{S_2^2 B\lambda_1\sin^2\theta}{\partial S_2/\partial\lambda_2} + \frac{-S_3S_2B^3\lambda_1^4\sin^2\theta}{\partial S_3/\partial\lambda_3}\right) \tag{20}$$

where θ is the crack orientation angle.

Note that the number of cycles to failure keeps the same form as in Section 3.1, see Eqs. (14) and (15).

The developed model was implemented into the commercial finite element (FE) code MSC.Marc via a subroutine to simulate rubber structures subjected to multiaxial loadings. For each increment, the subroutine is applied at every material integration point of each element. The angle of the virtual crack θ, used to compute the CED at each increment, is calculated by sweeping θ between 0° and 180° and keeping the θ value which maximizes the CED. The fatigue predictor given by Eq. (20) is extracted in the region of the specimen where it is maximal. It was observed that the maximum value is located in the smallest cross-section and that whatever the kind of loading. The maximum equivalent stress is then used to compute the fatigue life by using the formula (14).

The aim of the following section is to demonstrate that the proposed model is an efficient tool to predict the high-cycle fatigue life of SBR.

5. Results and discussion

Fatigue life is plotted in Fig. 7 as a function of the new equivalent stress defined by Eq. (20). The damage parameters a and A of Eq. (14) are identified in the same manner than that described in Section 3.2 by using the tensile fatigue tests. The least square method presented in Fig. 7 using Eq. (14) gives the following values for the damage parameters: $a = 4.15$ and $A = 6.22$ MPa. It is clearly highlighted that using the new equivalent stress as a fatigue parameter the model is able to unify the experimental data obtained under different loading paths. By using the damage parameters a and A derived from tensile tests, the predicted values of the fatigue life are slightly underestimated in the case of torsion tests. In this case, the experimental values of the number of cycles to failure perhaps suffer of a lack of accuracy. Indeed, the fatigue life is assumed to be the value when the initiated crack reaches 1 mm. The measurement of the crack length, operated in a visual manner, is not sufficiently accurate and some kind of discrepancy could be therefore generated that involves a scattering in the corresponding fatigue life values. Moreover, under torsion the crack propagation velocity is relatively small, so we can conclude that a small increment in crack length corresponds to a large increase of the number of cycles. It should be noticed that for some tested samples, the crack was superior to 1 mm before the test was stopped and it was referred to the global axial or torque responses to correct the cycle number. Another source of scattering could be due to self-heating generally observed when dealing with fatigue of rubbers and which was completely neglected in the proposed developments.

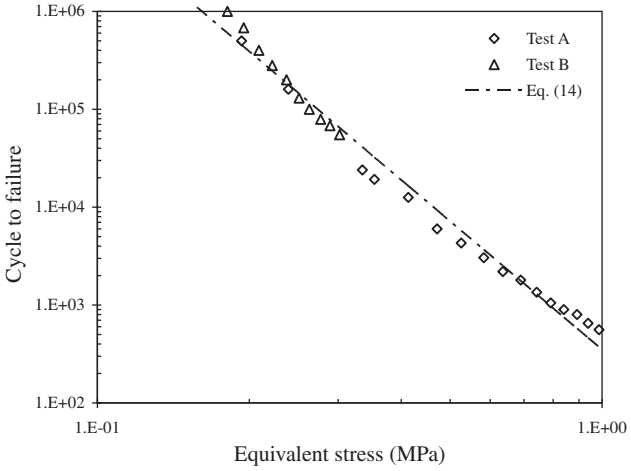

Fig. 7. Fatigue life of SBR in terms of the equivalent stress calculated using Eq. (20).

Beyond all the above-mentioned reasons to explain the scattering, there is another one which could be easily accounted for in the model. Indeed, one could introduce a threshold value of the equivalent stress corresponding to the endurance limit for the material. This modification is introduced by adding a threshold damage strain energy release rate y_{th} in the dissipation potential φ^* given by Eq. (3). The term y_{th} is written in the same way as the damage strain energy release rate y. A new formulation of the dissipation potential φ^* is then provided:

$$\varphi^* = \frac{A}{a+1}\left(\frac{-y + y_{th}}{A}\right)^{a+1} \tag{21}$$

The fatigue life is therefore rewritten as follows:

$$N_f = \frac{A^a}{1+a}(S_{eq} - S_{th})^{-a} \tag{22}$$

where S_{eq} is the equivalent stress given by Eq. (20), S_{th} is a threshold corresponding to the equivalent stress value below which the lifetime is theoretically unlimited, a and A as already mentioned are fatigue parameters identified from tensile fatigue tests ($a = 3.33$ and $A = 9.08$ MPa). In this work, S_{th} was experimentally estimated from a uniaxial tension fatigue test. Under a stretch amplitude of $\lambda_1 = 1.18$, no crack nucleation have been observed after cycling up to 5.10^6 cycles. This stretch value is supposed to be the endurance limit and used to calculate S_{th}. The fatigue life is plotted as a function of $S_{eq} - S_{th}$ in Fig. 8. It is clearly shown that introducing a threshold improves the predictive capability of the model.

Using these identified values Fig. 9 presents a comparison between the predictions of the proposed model and the experimental fatigue life data under constant amplitude loading conditions corresponding to tests A, B and C. The data are plotted in a diagram with the experimental fatigue life as ordinate and the predicted life as abscissa. The data are arranged around the median line proving the validity of our model.

Moreover, in order to check further its predictive capability, the criterion was also compared to more discriminant experimental data issued from loading conditions D. In order to take into account the nonlinear damaging, high then low loading (HL) and low then

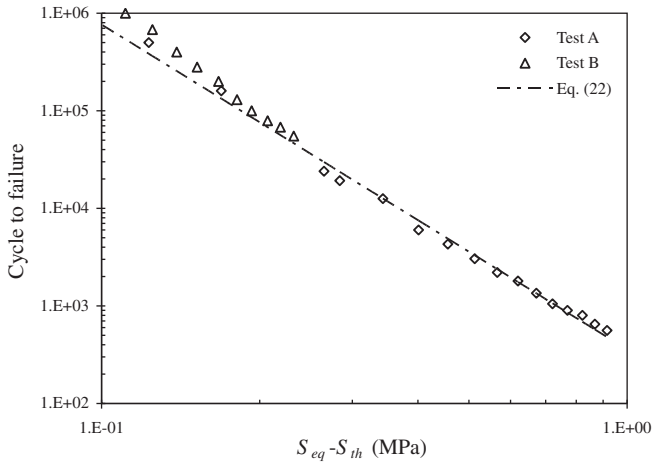

Fig. 8. Fatigue life of SBR in terms of the difference between equivalent and threshold stresses $S_{eq} - S_{th}$ calculated using Eq. (20).

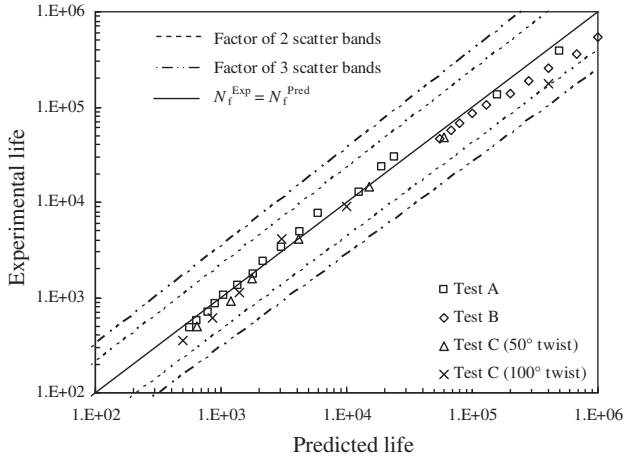

Fig. 9. Comparison between predicted and experimental fatigue life results (see Table 2 for the signification of test codes).

high (LH) loading were applied. It is worth noticing that LH configurations lead to higher fatigue duration than HL ones. The results are shown in Fig. 10. Again, it can be observed a quite good agreement between the predicted and experimental values. Note that in this case, the predictive values are conservative, so that security is preserved when designing rubber components by using our approach.

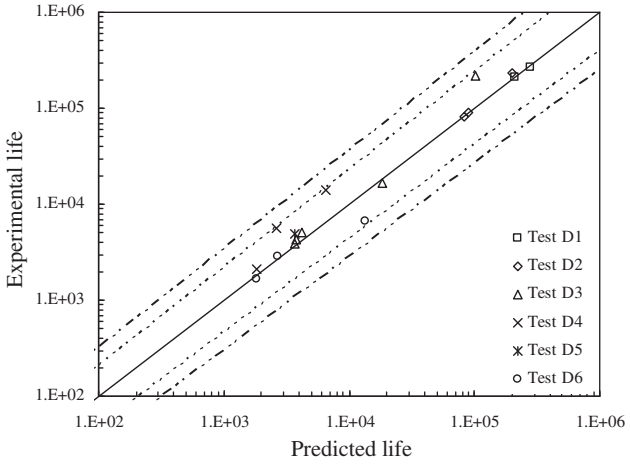

Fig. 10. Comparison between predicted and experimental fatigue life results for variable amplitude tests (see Table 3 for the signification of test codes).

6. Conclusion

In the present paper, using a CDM approach (Lemaitre and Chaboche, 1994) coupled with the CED (Mars, 2001, 2002) a new model for the fatigue life prediction of rubber-like materials under multiaxial loading conditions was proposed. Inherent to its mathematical construction, the developed CDM/CED model is both a criterion and an accumulative damage model. Fatigue tests achieved on the SBR material under constant and variable amplitude loading conditions allowed to check the relevance of the model. A satisfactory agreement was clearly pointed out. The predictive capability of the model was improved by introducing a threshold value for the equivalent stress corresponding to the endurance limit below which the fatigue life is considered as unlimited.

Three damage parameters are required in the model in addition to the constitutive law parameters. The parameters a and A are determined by a simple linear regression method on tensile fatigue tests and the parameter S_{th} is experimentally estimated under the same loading condition. This makes this model as a very attractive one, easy to implement in a FE code for designing more complex structures.

It could be necessary in the future to include some specific problems inherent to fatigue of rubbers such as self-heating which could be different from a specimen geometry to another.

Acknowledgement

The authors gratefully acknowledge the International Campus on Safety and Intermodality in Transportation, and the French ministry of higher education and research for its financial support. They also gratefully acknowledge the Trelleborg Group for providing the SBR samples.

Appendix A. Basic equations of CED concept

In the context of hyperelasticity, it seems natural to define the increment of total SED dW as follows:

$$dW = \frac{\rho}{\rho_0}\mathbf{S}d\mathbf{E} \tag{A.1}$$

where ρ/ρ_0 is the ratio of the deformed mass density to the undeformed mass density (for an incompressible material this ratio is taken equal to 1), $\mathbf{S}$ is the second Piola–Kirchhoff stress tensor and $\mathbf{E}$ is the Green–Lagrange strain tensor.

Mars (2001, 2002) reformulated for finite strains the increment of CED dW_c in the infinitesimal strain framework as[2]:

$$dW_c = \frac{\rho}{\rho_0}\frac{\mathbf{R}^T\mathbf{S}d\mathbf{E}\mathbf{C}^{-1}\mathbf{R}}{\mathbf{R}^T\mathbf{C}^{-1}\mathbf{R}} \tag{A.2}$$

in which $\mathbf{C}$ is the right Cauchy–Green strain tensor, $\mathbf{R}$ is the unit vector in the undeformed configuration defined (in a plan problem) in the following form: $\mathbf{R} = (\cos\theta, \sin\theta, 0)$ where θ is the crack orientation angle. The cracking plan is generally perpendicular to the direction of the maximum principal tensile strain.

[2] A mistake concerning the normal vector in the undeformed configuration is present in the formulation of Mars (2001, 2002) and Eq. (A.2) corresponds to the formulation corrected by Zine (2006).

In the principal directions, the deformation gradient tensor **F**, for incompressible materials, can be written as follows:

$$\mathbf{F} = \mathrm{diag}\left(\lambda_1, B\lambda_1, B^{-1}\lambda_1^{-2}\right) \tag{A.3}$$

where $B = \lambda_2/\lambda_1$ is the biaxiality ratio defined as the ratio between the second and first principal stretches.

In addition, the right Cauchy–Green strain tensor **C** and the Green–Lagrange strain tensor **E** can be respectively expressed in the following forms:

$$\begin{aligned}\mathbf{C} &= \mathbf{F}^{\mathbf{T}}\mathbf{F} = \mathrm{diag}\left(\lambda_1^2, B^2\lambda_1^2, B^{-2}\lambda_1^{-4}\right)\\ \mathbf{E} &= \frac{1}{2}(\mathbf{C}-\mathbf{I}) = \frac{1}{2}\mathrm{diag}\left(\lambda_1^2-1, B^2\lambda_1^2-1, B^{-2}\lambda_1^{-4}-1\right)\end{aligned} \tag{A.4}$$

Using Eqs. (A.2), (A.3) and (A.4) the CED formulation can be generalized as:

$$dW_c = \frac{1}{2}\frac{d\left(\lambda_1^2-1\right)\cos^2\theta S_1 + \frac{d\left(B^2\lambda_1^2-1\right)}{B^2}\sin^2\theta S_2}{\left(\cos^2\theta + B^{-2}\sin^2\theta\right)} \tag{A.5}$$

The crack orientation angle θ used in our calculation is the one which maximized the ratio W_c/W. Eq. (A.5) can be also reformulated, in partial derivative form, as:

$$dW_c = \frac{\partial W_c}{\partial\lambda_1}d\lambda_1 + \frac{\partial W_c}{\partial\lambda_2}d\lambda_2 + \frac{\partial W_c}{\partial\lambda_3}d\lambda_3 \tag{A.6}$$

where

$$\begin{aligned}\frac{\partial W_c}{\partial\lambda_1} &= \frac{\lambda_1 S_1\cos^2\theta}{\cos^2\theta + B^{-2}\sin^2\theta}\\ \frac{\partial W_c}{\partial\lambda_2} &= \frac{B\lambda_1 S_2\sin^2\theta}{\cos^2\theta + B^{-2}\sin^2\theta}\\ \frac{\partial W_c}{\partial\lambda_3} &= \frac{-B^3\lambda_1^4 S_2\sin^2\theta}{\cos^2\theta + B^{-2}\sin^2\theta}\end{aligned} \tag{A.7}$$

References

Abraham, F., Alshuth, T., Jerrams, S., 2005. The effect of minimum stress and stress amplitude on the fatigue life of non strain crystallising elastomers. Mater. Des. 26, 239–245.

Äit-Hocine, N., Naït-Abdelaziz, M., Mesmacque, G., 1998. Experimental and numerical investigation on single specimen methods of determination of *J* in rubber materials. Int. J. Fract. 94, 321–338.

Aït-Hocine, N., Hamdi, A., Naït-Abdelaziz, M., Heuillet, P., Zaïri, F., 2011. Experimental and finite element investigation of void nucleation in rubber-like materials. Inter. J. Solids Struct. 48, 1248–1254.

André, N., Cailletaud, G., Piques, R., 1999. Haigh diagram for fatigue crack initiation prediction of natural rubber components. Kaut. Gummi Kunst. 52, 120–123.

Ayoub, G., Naït-Abdelaziz, M., Zaïri, F., Gloaguen, J.M., 2010. Multiaxial fatigue life prediction of rubber-like materials using the continuum damage mechanics approach. Proc. Eng. 2, 985–993.

Ayoub, G., Zaïri, F., Naït-Abdelaziz, M., Gloaguen, J.M., 2011. Modeling the low-cycle fatigue behavior of visco-hyperelastic elastomeric materials using a new network alteration theory: application to styrene-butadiene rubber. J. Mech. Phys. Solids 59, 473–495.

Boyce, M.C., Arruda, E.M., 2000. Constitutive models of rubber elasticity: a review. Rubber Chem. Tech. 73, 504–523.

Cadwell, S.M., Merrill, R.A., Sloman, C.M., Yost, F.L., 1940. Dynamic fatigue life of rubber. Ind. Eng. Chem. 12, 19–23.

Chadwick, P., 1975. Applications of an energy-momentum tensor in non-linear elastostatics. J. Elast. 5, 249–258.

Dorfmann, A., Muhr, A., 1999. Constitutive Models for Rubber. A.A. Balkema, Rotterdam.

Eshelby, J.D., 1951. The force on an elastic singularity. Phil. Trans. R. Soc. Lond. A244, 87–112.

Fielding, J.H., 1943. Flex life and crystallization of synthetic rubber. Ind. Eng. Chem. 35, 1259–1261.

Gent, A.N., Lindley, P.B., Thomas, A.G., 1964. Cut growth and fatigue of rubbers. I. The relationship between cut growth and fatigue. J. Appl. Polym. Sci. 8, 455–466.

Griffith, A.A., 1920. The phenomena of rupture and flow in solids. Phil. Trans. R. Soc. Lond. A221, 163–198.

Harbour, R.J., Fatemi, A., Mars, W.V., 2008. Fatigue life analysis and predictions for NR and SBR under variable amplitude and multiaxial loading conditions. Int. J. Fatigue 30, 1231–1247.

Kachanov, LM., 1958. Time of the rupture process under creep conditions. Izv. Akad. Nauk. S.S.R. Otd. Tech. Nauk. 8, 26–31.

Klenke, D., Beste, A., 1987. Ensurance of the fatigue life of metal–rubber components. Kaut. Gummi Kunst. 40, 1067–1071.

Lee, M.P., Moet, A., 1993. Analysis of fatigue crack propagation in NR/BR rubber blend. Rubber Chem. Tech. 66, 304–316.

Lemaitre, J., Chaboche, J.L., 1994. Mechanics of Solid Materials. Cambridge University Press, Cambridge.

Mars, W.V. 2001. Multiaxial Fatigue of Rubber. Ph.D. Thesis, University of Toledo, USA.

Mars, W.V., 2002. Cracking energy density as a predictor of fatigue life under multiaxial conditions. Rubber Chem. Tech. 75, 1–17.

Mars, W.V., Fatemi, A., 2002. A literature survey on fatigue analysis approaches for rubber. Int. J. Fatigue 24, 949–961.

Maugin, G.A., 1993. Material Inhomogeneities in Elasticity. Chapman and Hall, London.

Miner, M.A., 1945. Cumulative damage in fatigue. J. Appl. Mech. 12, 159–164.

Ogden, RW., 1972. Large deformation isotropic elasticity: on the correlation of theory and experiment for incompressible rubberlike solids. Proc. R. Soc. Lond. A326, 565–584.

Rice, J.R., 1968. A path independent integral and the approximate analysis of strain concentration by notches and cracks. J. Appl. Mech. 35, 379–386.

Rivlin, R.S., Thomas, A.G., 1953. Rupture of rubber. I. Characteristic energy for tearing. J. Polym. Sci. 10, 291–318.

Ro, H.S. 1989. Modeling and Interpretation of Fatigue failure Initiation in Rubber Related to Pneumatic Tires. Ph.D. Thesis, University of Purdue, USA.

Roach, J.F. 1982. Crack Growth in Elastomers Under Biaxial Stresses. Ph.D. Thesis, University of Akron, USA.

Roberts, B.J., Benzies, J.B., 1977. The relationship between uniaxial and equibiaxial fatigue in gum and carbon black filled vulcanizates. Proc. Rubbercon'77 2, 1–13.

Saintier, N., Cailletaud, G., Piques, R., 2006. Crack initiation and propagation under multiaxial fatigue in a natural rubber. Int. J. Fatigue 28, 61–72.

Sun, C., Gent, A., Marteny, P., 2000. Effect of fatigue step loading sequence on residual strength. Tire Sci. Tech. 28, 196–208.

Verron, E., Andriyana, A., 2008. Definition of a new predictor for multiaxial fatigue crack nucleation in rubber. J. Mech. Phys. Solids 56, 417–443.

Wang, B., Lu, H., Kim, G.H., 2002. A damage model for the fatigue life of elastomeric materials. Mech. Mater. 34, 475–483.

Wöhler, A., 1867. Wöhler's experiments on the strength of metals. Engineering 4, 160–161.

Zine, A. 2006. Fatigue multiaxiale des élastomères: vers un critère de dimensionnement unifié. Ph.D. Thesis (in French), University of Lille, France.

Zine, A., Benseddiq, N., Naït-Abdelaziz, M., Äit-Hocine, N., Bouami, D., 2006. Prediction of rubber fatigue life under multiaxial loading. Fat. Fract. Eng. Mater. Struct. 29, 267–278.